Visual Chatter in the Real World

Shree K. Nayar[1], Gurunandan Krishnan[1], Michael D. Grossberg[2], and Ramesh Raskar[3]

[1] Columbia University, New York, NY
nayar@cs.columbia.edu, gkguru@cs.columbia.edu
[2] City University of New York, New York, NY
grossberg@cs.ccny.cuny.edu
[3] MERL, Cambridge, MA
raskar@merl.com

Abstract. We present fast methods for separating the direct and global illumination components of a scene measured by a camera and illuminated by a light source. In theory, the separation can be done with just two images taken with a high frequency binary illumination pattern and its complement. In practice, a larger number of images are used to overcome the optical and resolution limitations of the camera and the source. The approach does not require the material properties of objects and media in the scene to be known. However, we require that the illumination frequency is high enough to adequately sample the global components received by scene points. We present separation results for scenes that include complex interreflections, subsurface scattering and volumetric scattering. The computed direct and global images provide interesting insights into how real-world objects interact with light as well as optically interact with each other (hence the term "visual chatter"). All the measurement results reported here, as well as several others, can be viewed as high resolution images at *http://www1.cs.columbia.edu/CAVE/projects/separation/separation.php*.

1 Introduction

When a scene is lit by a source of light, the radiance of each point in the scene can be viewed as having two components, namely, direct and global. The direct component is due to the direct illumination of the point by the source. The global component is due to the illumination of the point by other points in the scene. Consider the scene point P shown in Fig. 2. The light ray A represents its direct illumination by the source and hence is the sole cause for the direct component of the radiance measured by the camera. The rays B, C, D and E are received by P from other points in the scene, and together they contribute to the global component of its radiance measured by the camera. These global illumination light rays are caused by different physical phenomena that are common in the real world. Ray B represents the interreflection of light between scene points; ray C results from subsurface scattering within the medium beneath the surface; ray D is due to volumetric scattering by a participating medium in the scene; and ray E is due to diffusion of light by a translucent surface.

M. Kaneko and Y. Nakamura (Eds.): Robotics Research, STAR 66, pp. 13–24.
springerlink.com

(a) Scene (b) Direct Component (c) Global Component

Fig. 1. (a) A scene lit by a single source of light. The scene includes a wide variety of physical phenomena that produce complex global illumination effects. We present several methods for separating the (b) direct and (c) global illumination components of the scene using high frequency illumination.

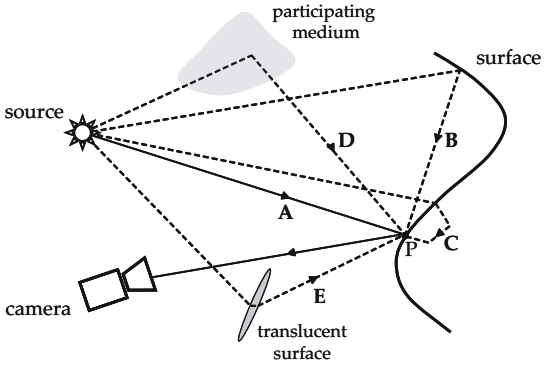

Fig. 2. The radiance of scene point is due to direct illumination of the point by the source (A) and global illumination due to other points in the scene. The global illumination can arise from interreflections (B), subsurface scattering (C), volumetric scattering (D) and translucency (E). Separation of the direct and global components of measured radiance is useful as these components convey different properties of the scene.

It is highly desirable to have a method for measuring the direct and global components of a scene, as each component conveys important information about the scene that cannot be inferred from their sum. For instance, the direct component gives us the purest measurement of how the material properties of a scene point interact with the source and camera. Therefore, a method that can measure just the direct component can be immediately used to enhance a wide range of scene capture techniques that are used in computer vision and computer graphics. The global component conveys the complex optical interactions between different objects and media in the scene. We know that it is the global component that makes photorealistic rendering a hard and computationally intensive problem. A measurement of this component could provide new insights into these interactions that in turn could aid the development of more efficient rendering algorithms. Furthermore, measurement of the direct and global

components can enable new types of image manipulations that are more faithful to the physical laws that govern scattering.

The goal of this paper is to develop efficient methods for separating the direct and global components of a scene lit by a single light source and viewed by a camera. One way to measure the global component is to illuminate each point of the scene independently and capture an image to determine the contribution of the point to all other points, as recently proposed in [20]. While this approach is valid from a theoretical standpoint, it becomes prohibitively expensive for large and complex scenes. We show that the direct and global components at all scene points can be efficiently measured by using high frequency illumination patterns. This approach does not require the scattering properties of the scene points to be known. We only assume that the global contribution received by each scene point is a smooth function with respect to the frequency of the lighting. This assumption makes it possible, in theory, to do the separation by capturing just two images taken with a dense binary illumination pattern and its complement. In practice, due to the resolution limits imposed by the source and the camera, a larger set of images (25 in our setting) is used. We show separation results for several scenes that include diffuse and specular interreflections, subsurface scattering due to translucent surfaces and volumetric scattering due to dense media. We have also measured the two components for a 3D texture as a function of lighting direction. We conclude the paper with a discussion on several extensions of our approach that are planned for the future.

2 Related Work

There has been limited work on separating the direct and global illumination components of a scene from images. Classical shape-from-brightness algorithms, such as photometric stereo [24], do not account for global illumination due to interreflections and hence produce incorrect shape and reflectance estimates for scenes with concavities. For Lambertian surfaces, Nayar et al.[17] analyzed the properties of the incorrect shape and reflectance produced by photometric stereo and showed that the actual shape and reflectance can be recovered from the incorrect ones. This recovery process implicitly separates the direct and global components of the scene. However, this approach is hard to extend to non-Lambertian scenes with complex geometries of the type we are interested in.

In the case of pure interreflections produced by any opaque surface, the direct and global components can be interpreted in a simple manner. The direct component is due to a single reflection at the surface, while the global component is due to multiple reflections. An interesting theoretical decomposition based on this interpretation was recently proposed by Seitz et al. [20]. They also presented a method for estimating the interreflection contribution due to any given number of reflections. While the decomposition itself is applicable to surfaces with arbitrary BRDF, the method for estimating the decomposition is based on the Lambertian assumption. Moreover, this method requires a very large number of

images to be acquired as it needs to know the photometric coupling between all pairs of scene points.

In order to separate the illumination components of arbitrary scenes, one needs to go beyond the realm of interreflections and be able to handle more complex phenomena such as subsurface scattering in translucent objects and volumetric scattering by participating media. A general approach to this problem is to estimate the dependence of the light field [6, 14] of a scene on an arbitrary illumination field. This dependence is expressed as a linear transformation called a transport matrix. Due to its enormous dimensionality, estimation of the transport matrix requires a very large number of images and illuminations. Several techniques have been proposed to reduce the number of images by using coded illumination fields [2, 15, 19, 21, 25, 26]. Even so, typically, several tens or even hundreds of images are needed to obtain acceptable estimates of the transport matrix. In our work, we do not aim to recover the entire transport matrix. Our goal is less ambitious – it is to separate the appearance of a scene lit by a single source into its direct and global components. In this setting, we show that the separation can be done with a very small number of images.

3 Theory of Fast Separation

3.1 Definitions for Direct and Global Illumination

Consider a surface viewed by a camera and illuminated by a point source, as shown in Fig. 3(a). Let us assume that the source generates a set of illumination rays, each ray corresponding to a single source element, as in the case of a digital projector. We assume that each point of the surface could cause a significant scattering event in the direction of the camera if lit by the source. The radiance of a surface point measured by the camera due to such a scattering event is referred to as the *direct component*, L_d. The exact value of the direct component is determined by the BRDF of the surface point, which can be arbitrary[1]. For our separation method to work, we assume that each camera pixel can observe at most one significant scattering event, i.e. two different source elements cannot produce a direct component along a camera pixel's line of sight[2].

The remaining radiance measured by the camera pixel is referred to as the *global component*, L_g. In computer graphics, this term is typically used to denote interreflections – light received by a surface point after reflection by other scene points. Here, we are using a more general definition. In addition to interreflections, the global illumination received by the surface point may be due to

[1] Since, in practice, cameras and sources have finite resolutions, the direct component is the aggregate of all the scattering that occurs within the volume of intersection between the fields of view of the camera pixel that observes the surface point and the source element that illuminates it.

[2] A scenario that violates this assumption is the case of a transparent (and yet reflective) surface in front of another surface, where a camera pixel's line of sight could produce two significant scatterings due to different source elements (pixels in the case of a projector).

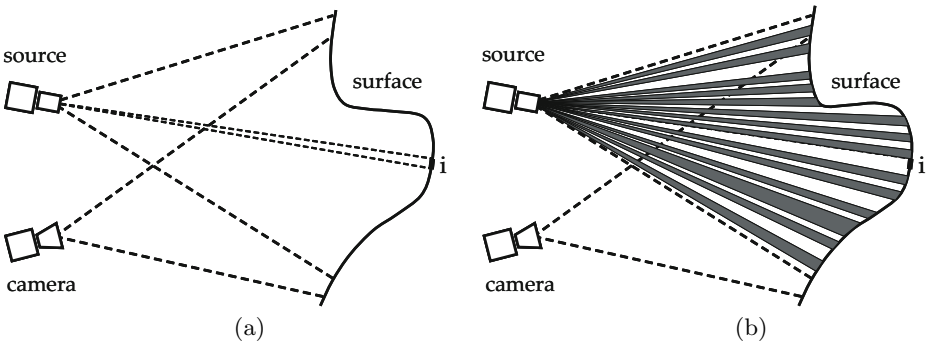

Fig. 3. (a) A simple scenario where the radiance of each patch i includes a direct component due to scattering of light incident directly from the source and a global component due to light incident from other points in the scene. (b) When the source radiates a high frequency binary illumination pattern, the lit patches include both direct and global components while the unlit patches have only a global component. In theory, two images of the scene taken with such an illumination pattern and its complement are sufficient to estimate the direct and global components for all patches in the scene.

volumetric scattering, subsurface scattering or even light diffusion by translucent surfaces (see Fig. 2). The case of diffusion by a translucent surface works similarly to interreflections. In the case of volumetric scattering, the global component arises from the illumination of the surface point by light scattered from particles suspended in a participating medium. In the case of subsurface scattering, the surface point receives light from other points within the surface medium. Finally, the global component also includes volumetric and subsurface effects that may occur within the camera pixel's field of view but outside the volume of intersection between the fields of view of the pixel and the source element that produces a significant scattering event at the pixel. These are considered to be global effects as they are not significant scattering events caused by individual source elements[3].

In all cases, the total radiance measured at a camera pixel is the sum of the direct and global components:

$$L = L_d + L_g \,. \tag{1}$$

3.2 The Nature of the Light Source

In our work, we restrict ourselves to the use of a single camera and a single source. While we will use a point source to describe our separation method,

[3] This claim does not hold true when the source and the camera are co-located. In this special case, the field of view of each camera pixel is illuminated by a single source element and hence the volumetric and subsurface scattering effects within the pixel's field of view will indeed be significant scattering events and hence appear in the direct component.

this is not a strict requirement. We only require that each point in the scene be directly illuminated by at most one source element. In other words, the light rays corresponding to the source elements should not intersect within the working volume of the setup used to perform the separation. Any source (point or extended) that satisfies this condition may be used.

3.3 Separation Using High Frequency Illumination

Let us assume that the scene in Fig. 3(a) includes a single opaque surface of arbitrary BRDF immersed in a non-scattering medium so that the global component arises solely from interreflections. However, our analysis of this case is also applicable to other phenomena such as subsurface and volumetric scattering.

Let us divide the surface into a total of N patches, M of which are directly visible to the source. Each of these M visible patches corresponds to a single pixel of the source. We denote the radiance of the patch i measured by the camera c as $L[c,i]$, and its two components as $L_d[c,i]$ and $L_g[c,i]$, so that $L[c,i] = L_d[c,i] + L_g[c,i]$. The global component of i due to interreflections from all other surface patches can be written as:

$$L_g[c,i] = \sum_{j \in P} A[i,j]\, L[i,j]\,, \tag{2}$$

where, $P = \{j | 1 \leq j \leq N, j \neq i\}$. $L[i,j]$ is the radiance of patch j in the direction of patch i and $A[i,j]$ incorporates the BRDF of i as well as the relative geometric configuration of the two patches[4]. We can further decompose $L_g[c,i]$ into two components as $L_g[c,i] = L_{gd}[c,i] + L_{gg}[c,i]$, where $L_{gd}[c,i]$ is due to the direct component of radiance from all scene patches and $L_{gg}[c,i]$ is due to the global component of radiance from all scene patches:

$$L_{gd}[c,i] = \sum_{j \in P} A[i,j] L_d[i,j]\ , \qquad L_{gg}[c,i] = \sum_{j \in P} A[i,j]\, L_g[i,j]\,. \tag{3}$$

Now let us assume that only a fraction α of the source pixels are activated and that these activated pixels are well-distributed over the entire scene to produce a high frequency illumination pattern, as shown in Fig. 3(b). The set of illuminated patches can be denoted as $Q = \{k | k \in N \text{ and } lit(k) = 1\}$, where the function *lit* indicates whether a patch is illuminated or not. Then, the above components become:

$$L_{gd}{}^{+}[c,i] = \sum_{j \in Q} A[i,j]\, L_d[i,j], \;\; L_{gg}{}^{+}[c,i] = \sum_{j \in P} A[i,j]\, L_g{}^{+}[i,j]. \tag{4}$$

Note that $L_{gd}{}^{+}[c,i]$ differs from $L_{gd}[c,i]$ only in that the lit αM patches rather than all the M patches have a direct component and hence make a contribution.

[4] Details on the form of $A[i,j]$ can be found in [1, 13, 12, 9, 3, 17, 20]. In our work, the exact form of $A[i,j]$ is not relevant as it not used explicitly during separation.

Therefore, if the geometry and reflectance term $A[i,j]$ and the direct component $L_d[i,j]$ are smooth with respect to the frequency of the illumination pattern, we have:

$$L_{gd}{}^{+}[c,i] = \alpha L_{gd}[c,i]\,. \tag{5}$$

A brief frequency domain analysis of the illumination frequency that makes the above relation valid is provided in [18].

Now, let us consider the second term, $L_{gg}{}^{+}[c,i]$. Since $L_g{}^{+}[i,j]$ in Equation (4) is the result of higher orders of interreflection than $L_{gd}{}^{+}[c,i]$, it is even smoother and hence less affected by the non-uniformity of the illumination. However, it is directly proportional to the average power of the illumination, which is reduced by α in the case of the high frequency pattern. Therefore, $L_g{}^{+}[i,j] = \alpha L_g[i,j]$ and we get:

$$L_{gg}{}^{+}[c,i] = \alpha L_{gg}[c,i]\,. \tag{6}$$

Consider two captured images of the scene, where, in the first image L^+ the scene is lit with high frequency illumination that has fraction α activated source pixels and in the second image L^- it is lit with the complementary illumination that has fraction $1-\alpha$ activated source pixels. If the patch i is lit directly by the source in the first image then it is not lit by the source in the second image, and we get:

$$L^+[c,i] = L_d[c,i] + \alpha L_g[c,i]\,, \quad L^-[c,i] = (1-\alpha)L_g[c,i]\,. \tag{7}$$

Therefore, if we know α, we can compute the direct and global components at each camera pixel from just two images. Thus far, we have assumed that when a source pixel is not activated it does not generate any light. In the case of a projector, for example, this is seldom completely true. If we assume the brightness of a deactivated source element is a fraction b, where $0 \le b \le 1$, of an activated element, then the above expressions can be modified as:

$$\begin{aligned} L^+[c,i] &= L_d[c,i] + \alpha L_g[c,i] + b(1-\alpha)L_g[c,i]\,, \\ L^-[c,i] &= b\,L_d[c,i] + (1-\alpha)L_g[c,i] + \alpha b L_g[c,i]\,. \end{aligned} \tag{8}$$

Again, if α and b are known, the separation can be done using just two images. Note that if α is either close to 1 or 0, the scene will be lit (sampled) very sparsely in one of the two images. Since we wish to maximize the sampling frequency of the illumination in both images, a good choice is $\alpha = \frac{1}{2}$. In this case, we get:

$$\begin{aligned} L^+[c,i] &= L_d[c,i] + (1+b)\frac{L_g[c,i]}{2}\,, \\ L^-[c,i] &= bL_d[c,i] + (1+b)\frac{L_g[c,i]}{2}\,. \end{aligned} \tag{9}$$

Based on the above results, a variety of separation methods have been developed and are described in [18]. In each case, we will record a set of brightness values at each camera pixel and use L_{max} and L_{min} to denote the maximum and minimum of these values. In the above case of two images taken with $\alpha = \frac{1}{2}$, $L^+ \ge L^-$ and hence $L_{max} = L^+$ and $L_{min} = L^-$.

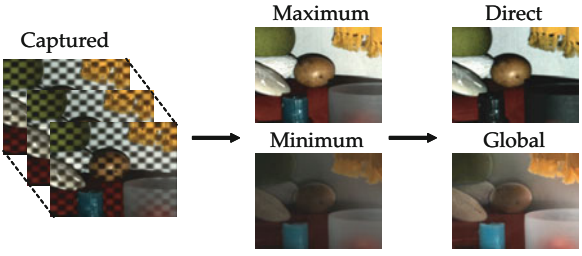

Fig. 4. The steps involved in the computation of direct and global images using a set of shifted checkerboard illumination patterns.

A separation method which follows directly from the theory presented above, uses a high frequency checkerboard pattern and its complementary pattern for illumination. Unfortunately, it is difficult to obtain such ideal patterns using an off-the-shelf projector. To overcome this we take a larger number of images than the theory requires using shifted checkerboard patterns. The separation steps are illustrated in Fig. 4. At each pixel, the maximum and minimum measured brightnesses (L_{max}, L_{min}) are used to compute the direct and global estimates (L_d, L_g) using Equation 9.

Several variants of this method seek to minimize the number of images needed for separation. Using a sinusoid-based illumination pattern, the separation can be done using just three images taken by changing the phase of the pattern. When the resolution of the camera and the source are greater than the desired resolution of the direct and global images, the separation can be done with a single image by assuming neighboring scene points to have similar direct and global components. In the case of just a simple point light source, such as the sun, the source cannot be controlled to generate the required high frequency illumination patterns. In such cases, the shadow of a line or mesh occluder can be swept over the scene while it is captured by a video camera. The captured video can then be used to compute the direct and global components. A more detailed description of these variants is provided in [18].

4 Visual Chatter in the Real World

We now present separation results for a variety of real-world materials and objects (see Fig. 5 to Fig. 10). Note that each example highlights a specific physical phenomenon like interreflection, volumetric scattering or subsurface scattering. In each figure, the effects captured in the direct and global images are discussed in the caption. The examples shown here illustrate how real-world objects interact with light as well as optically interact with each other. Some of these interactions confirm our intuitions on how global illumination works. Others reveal surprising effects and provide new insights into the scattering properties of commonplace materials. All of the results presented here were obtained using the shifted checkerboard illumination pattern using a 1280x720 DLP projector and a 1024x728 color camera.

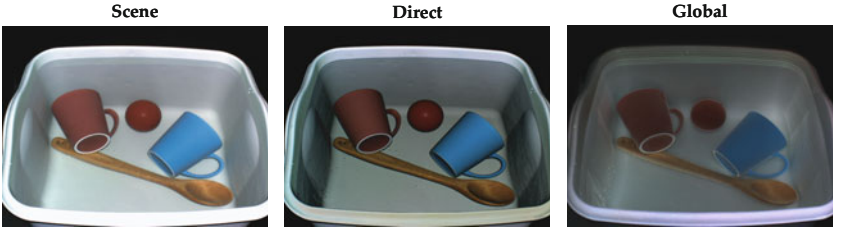

Fig. 5. Kitchen Sink: This scene includes objects in a sink filled with water. Since the water is clear it serves as a fully transparent medium and does not influence the scattering effects. It is worth noting that the computed direct image looks like a synthetic image rendered using a single-bounce rendering package such as OpenGL. All the interreflections between the sink and the objects are observed in the global image. Notice the strong interreflections at the edges and corners of the sink and the occluding boundaries of the curved objects.

Fig. 6. Translucent Colored Balls: The balls in this scene exhibit very strong subsurface scattering which causes them to "glow" under virtually any illumination [5, 11]. We see that all the subsurface scattering is captured in the global image. Perhaps, due to strong multiple scattering, the global images of the balls have very little shading, causing the balls to appear like flat discs (particularly, the green ball). On the other hand, the direct component reveals the spherical shapes of the balls and the roughness of their surfaces.

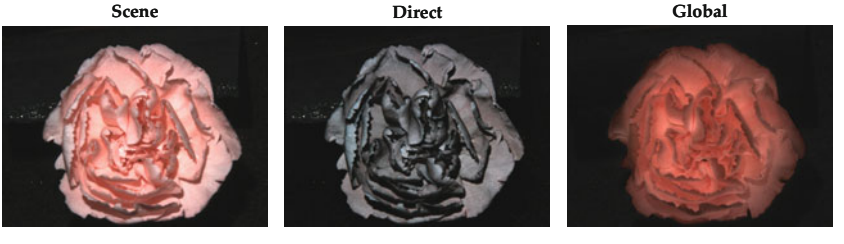

Fig. 7. Pink Carnation: In the case of this flower, we see that in the direct image the shadows cast by the petals on each other are strong and the petals themselves appear grayish and somewhat listless. As a result, the direct image looks more like that of a synthetic flower than a natural one. It is interesting to note that most of the color of the flower arises from global effects. These include the interreflection of light between the petals as well as the diffusion of light through the petals. Both these effects cause a "sharpening" of the spectral distribution of the light [4]. As a result, in this example, the color of the light gets more reddish after each bounce or diffusion.

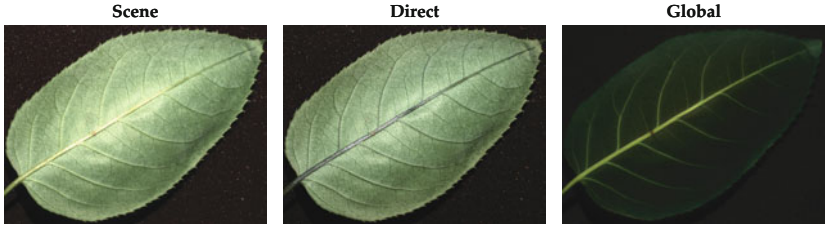

Fig. 8. Hybrid Tea Rose Leaf: Although the leaf is thin, it exhibits a noticeable global component over its entire area. This is because the entire leaf has a spongy mesophyll layer, beneath the upper epidermis and palisade mesophyll layers, that exhibits subsurface scattering. In particular, the global component is strong for the veins of the leaf. This is probably because the veins are translucent as they are made of vascular tissues that carry water, minerals and sap.

Fig. 9. Plastic Cup with Milky Water and Coin: In this example, the global image includes the volumetric scattering [1, 10] of light by the milky water (referred to as "airlight" in atmospheric optics [16]) in the cup as well as the secondary illumination of the copper coin by the milky water. The direct component includes the specular highlights on the copper coin due to direct illumination of the coin by the source. This component is attenuated (referred to as "direct transmission" in atmospheric optics [16]) by the milky water as it makes its way to the camera. The wax candle on the right has a strong subsurface scattering component. As a result, all of its color is captured in the global image and the direct image only includes the surface reflection (highlights) from the candle.

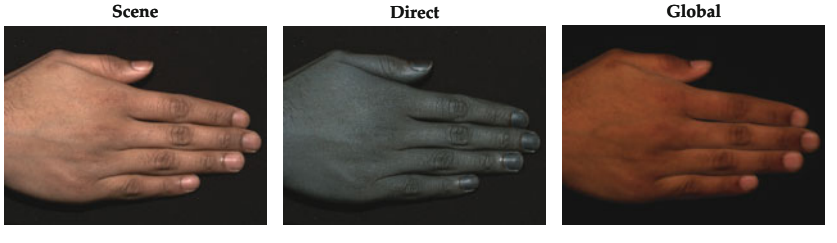

Fig. 10. Hand: Here, we show separation results for the hand of an Asian Indian male. Notice how the direct component mainly includes the surface reflection due to oils and lipids on the skin. It also reveals the details of the micro-geometry of the skin surface [23]. Most of the color of the skin comes from subsurface scattering, as seen in the global image [2, 7, 11, 22]. In contrast to the direct component, the global component does not reveal the roughness of the skin's surface and only includes albedo variations. The details of the geometry and optics of skin can be found in [8].

5 Discussion

We have developed efficient methods for separating the direct and global components of a scene lit by a single light source. Our separation approach is applicable to complex scenes with a wide variety of global illumination effects. To our knowledge, this is the first time the direct and global images of arbitrarily complex real-world scenes have been measured. These images reveal a variety of non-intuitive effects and provide new insights into the optical interactions between objects in a scene.

Our separation technique only produces the total global component at each scene point and not the photometric coupling between all pairs of scene points. We are looking into ways of using high frequency illuminations to estimate the complete transport matrix associated with a scene. This would lead to deeper insights into the photometric properties of real scenes and perhaps even more powerful methods for creating novel images. We have also assumed that the direct component arises from a single dominant source and that all other sources contribute to the global component. It would be useful to extend our results to the case of multiple sources without having to activate the sources in a sequential fashion.

Acknowledgments

This research was supported in parts by a grant from the Office of Naval Research (No. N000140510188) and by Mitsubishi Electric Research Laboratory, Cambridge, MA. The authors thank Vijay Anand for his help with the coding of the separation method.

References

1. Chandrasekhar, S.: Radiative Transfer. Clarendon Press, Oxford (1950); reprinted by Dover Publications, New York (1960)
2. Debevec, P., Hawkins, T.C.T., Duiker, H., Sarokin, W., Sagar, M.: Acquiring the Reflectance Field of a Human Face. In: Proc. of SIGGRAPH, pp. 145–156. ACM Press, New York (2000)
3. Forsyth, D., Zisserman, A.: Reflections on Shading. IEEE Trans. on PAMI 13(7), 671–679 (1991)
4. Funt, B.V., Drew, M.S., Ho, J.: Color Constancy from Mutual Reflection. Int. Jour. of Comp. Vision 6(1), 5–24 (1991)
5. Goesele, M., Lensch, H., Lang, J., Fuchs, C., Seidel, H.: DISCO: Acquisition of Translucent Objects. In: Proc. of SIGGRAPH, pp. 835–844. ACM Press, New York (2004)
6. Gortler, S., Grzeszczuk, R., Szeliski, R., Cohen, M.: The Lumigraph. In: Proc. of SIGGRAPH, pp. 43–54. ACM Press, New York (1996)
7. Hanrahan, P., Krueger, W.: Reflection from Layered Surfaces due to Subsurface Scattering. In: Proc. of SIGGRAPH, pp. 165–174. ACM Press, New York (1993)
8. Igarashi, T., Nishino, K., and Nayar, S. K, The Appearance of Human Skin. Tech. Report, Dept. of Comp. Science, Columbia Univ. CUCS-024-05 (2005)

9. Immel, D., Cohen, M., Greenberg, D.: A Radiosity Method for Non-Diffuse Environments. In: Proc. of SIGGRAPH, pp. 133–142. ACM Press, New York (1986)
10. Ishimaru, A.: Wave Propagation and Scattering in Random Media. Academic Press, London (1978)
11. Jensen, H.: Realistic Image Synthesis Using Photon Mapping. AK Peters, Natick (2001)
12. Kajiya, J.T.: The Rendering Equation. In: Proc. of SIGGRAPH, pp. 143–150. ACM Press, New York (1986)
13. Koenderink, J., van Doorn, A.: Geometrical Modes as a General Method to Treat Diffuse Interreflections in Radiometry. In: JOSA, vol. 73, pp. 843–850 (1983)
14. Levoy, M., Hanrahan, P.: Light Field Rendering. In: Proc. of SIGGRAPH, pp. 31–42. ACM Press, New York (1996)
15. Lin, Z., Wong, T., Shum, H.: Relighting with the Reflected Irradiance Field: Representation, Sampling and Reconstruction. IJCV 49, 229–246 (2002)
16. Middleton, W.K.: Vision through the Atmosphere. Univ. of Tor. Press (1952)
17. Nayar, S., Ikeuchi, K., Kanade, T.: Shape from Interreflections. IJCV 6(3), 173–195 (1991)
18. Nayar, S.K., Krishnan, G., Grossberg, M.D., Raskar, R.: Fast Separation of Direct and Global Components of a Scene using High Frequency Illumination. In: Proc. of ACM SIGGRAPH, pp. 145–156 (July 2006)
19. Peers, P., Dutré, P.: Wavelet Environment Matting. In: Eurographics Symposium on Rendering, pp. 157–166. ACM Press, New York (2003)
20. Seitz, S., Matsushita, Y., Kutulakos, K.: A Theory of Inverse Light Transport. In: Proc. of ICCV, vol. II, pp. 1440–1447 (2005)
21. Sen, P., Chen, B., Garg, G., Marschner, S., Horowitz, M., Levoy, M., Lensch, H.: Dual Photography. ACM Trans. on Graph. 24, 745–755 (2005)
22. Tsumura, N., Ojima, N., Sato, K., Shiraishi, M., Shimizu, H., Nabeshima, H., Akazaki, S., Hori, K., Miyake, Y.: Image-based Skin Color and Texture Analysis/Synthesis by Extracting Hemoglobin and Melanin Information in the Skin. In: Proc. of SIGGRAPH, pp. 770–779. ACM Press, New York (2003)
23. Uchida, T., Komeda, T., Miyagi, M., Koyama, H., Funakubo, H.: Quantification of Skin Aging by Three-Dimensional Measurement of Skin Surface Contour. In: IEEE Int. Conf. Systems, Man, and Cybernetics (1996)
24. Woodham, R.: Photometric Method for Determining Surface Orientation from Multiple Images. Optical Engineering 19(1), 139–144 (1980)
25. Zhu, J., Yang, Y.: Frequency-based Environment Matting. In: Pacific Conf. on Comp. Graph. and Apps., pp. 402–410 (2004)
26. Zongker, D., Werner, D., Curless, B., Salesin, D.: Environment Matting and Compositing. In: Proc. of SIGGRAPH, pp. 205–214. ACM Press, New York (1999)